International Tables for Crystallography (2006). Vol. C, Chapter 6.3, pp. 599–608.

6.3. X-ray absorption

BY E. N. MASLEN

6.3.1. Linear absorption coefficient

When a monochromatic X-ray beam of intensity I_o travels a distance T through a homogeneous isotropic material, the intensity is reduced to a value

$$I = I_o \exp(-\mu T), \tag{6.3.1.1}$$

where μ is the total linear absorption coefficient. This expression can also be applied to X-ray absorption in crystalline solids provided the absorption is insensitive to the arrangement of the atoms in the unit cell. This holds to a good approximation in most cases. If it is assumed that the absorption processes are additive,

$$\mu = \frac{1}{V_c} \sum_{n=1}^{N_n} \sigma_n, \tag{6.3.1.2}$$

where V_c is the cell volume and there are N_n contributions to absorption per cell. σ_n is the absorption cross section for the nth contribution.

Of the processes that reduce the intensity of X-rays passing through matter, described in detail by Anderson (1984), photoelectric absorption, scattering, and extinction are important for the X-ray wavelengths used in crystallography.

6.3.1.1. *True or photoelectric absorption*

In photoelectric absorption, X-ray photons disappear completely. The absorption of each photon results in the ejection from the atom of an electron that carries excess energy away as kinetic energy. The corresponding linear photoelectric absorption cross section $\sigma_{\rm ph}$ is occasionally termed the cross section for 'fluorescence'.

Excitation of an electron from a low to a higher bound state also occurs. Such an electron can be excited only if the photon energy exceeds the gap to the nearest unoccupied level. For this reason, $\sigma_{\rm ph}$ varies abruptly in the manner shown in Fig. 6.3.1.1.

The probability of ejection of an electron is largest for a photon energy just sufficient for excitation. It is small if the energy greatly exceeds that required. With increasing atomic number Z, the absorption edges shift to shorter wavelengths. The ratio of the value of $\sigma_{\rm ph}$ for λ just below and just above the edge decreases with increasing Z, especially for the K edge.

The natural width of the resulting core-vacancy state sets a lower limit to the sharpness of the absorption edge (James, 1962). In some cases, such as the K edges for certain metals, the edge is substantially less sharp than that limit (Beeman & Friedman, 1939). Natural level widths are tabulated by Krause & Oliver (1979).

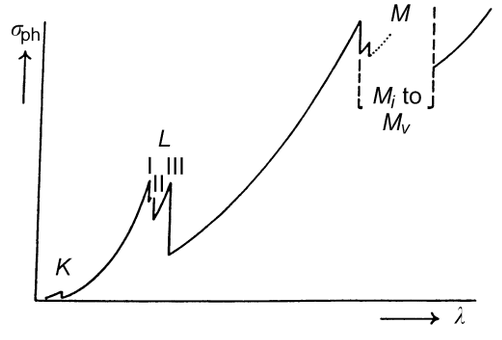

Fig. 6.3.1.1. Idealized diagram showing the variation of the photoelectric absorption coefficient $\sigma_{\rm ph}$ with wavelength λ.

The wavelength of the absorption edge for a given element shifts slightly with changes in the chemical environment of the absorbing atom. There is also fine structure in the absorption coefficient that depends, especially on the short-wavelength side, both on chemical composition and on temperature. The range of the larger effects in the fine structure is of the order of 10^{-3} Å for X-ray wavelengths of approximately 1 Å. This corresponds to a photon-energy range of tens of electron volts, whereas X-ray photon energies are of the order of 10 keV. Smaller effects in the fine structure cover a far greater range. These are observed in extended X-ray absorption fine structure (EXAFS) spectra up to 1 keV from the edge (see Section 4.2.3). However, these small terms are of limited relevance when measuring X-ray diffraction intensities.

6.3.1.2. *Scattering*

The X-ray photon is deflected from the original beam by collisions with atoms or electrons, the linear scattering cross section being $\sigma_{\rm sc}$. The total cross section

$$\sigma = \sigma_{\rm ph} + \sigma_{\rm sc} + \sigma', \tag{6.3.1.3}$$

where σ' is the combined cross section for all processes other than photoelectric absorption or scattering.

There are two types of scattering process, coherent (Rayleigh) scattering and incoherent (Compton) scattering as described in Section 6.1.1. Rayleigh scattering may be regarded as resulting from a collision between a photon and an atom as a whole. Because the effective mass of a photon is far less than that of an atom, the photon retains its original energy. In a frame with the atom at rest, the scattering is elastic – *i.e.* the photon wavelength is essentially unmodified.

Rayleigh scattering by isolated atoms increases monotonically with Z – the cross section is proportional to the square of the integral of the atomic scattering factor f. However, the photoelectric absorption cross section increases far more rapidly, so Rayleigh scattering is relatively more important for atoms with low atomic number.

The atomic Rayleigh cross sections decrease with λ. Although there are anomalies near absorption edges, these have a limited effect on σ because the Rayleigh scattering in these regions is small compared with the photoelectric cross section except for the lightest elements.

The cross section for Compton scattering depends on the state of the electrons involved in the collision, but for very short wavelengths the atomic Compton cross section is approximately proportional to the atomic number. It varies far more slowly with λ than either the photoelectric or the Rayleigh cross section.

6.3.1.3. *Extinction*

Because Rayleigh scattering is elastic, the scattering from different atoms may combine coherently, giving rise to interference, and hence to Bragg reflection from crystals.

For a crystal oriented so that there is no Bragg reflection, the interference reduces the scattered intensity far below the sum of the intensities that would be scattered by the atoms individually. For a strong Bragg reflection, on the other hand, the atomic scattering amplitudes add approximately in phase. The reduc-

tion in incident-beam intensity is many times larger than the sum of the squares of the individual atomic scattering powers.

An extreme case occurs in a perfect crystal, for which total reflection is possible. There is destructive interference with the incident beam producing a marked change in the index of refraction from its normal value of

$$n = 1 - \frac{\lambda^2 e^2}{2\pi mc^2} \sum_a N_a f_a(0), \qquad (6.3.1.4)$$

where e and m are the charge and mass of the electron. $f_a(0)$ is the scattering factor in the forward direction for an atom of type a and N_a is the number of atoms of that type per unit volume.

Thus, for strong reflections in near-perfect crystals, the Rayleigh scattering is affected by both crystal texture and beam direction. This reduction of primary-beam intensity due to the Rayleigh scattering is usually included, along with other specimen-dependent factors affecting diffracted-beam intensity, in the analysis of extinction.

6.3.1.4. *Attenuation (mass absorption) coefficients*

Since the reduction of intensity depends on the quantity of matter traversed by the beam, the absorption coefficient is often expressed on a mass basis by dividing by the density ρ_m. μ/ρ_m defines the attenuation coefficient.

The determination of attenuation coefficients to high precision is possible only when contributions from all different scattering processes are analysed in detail. To a level of accuracy appropriate to most experiments, however, the coefficient can be determined from the atomic cross sections for scattering and photoelectric absorption. Ideally, absorption corrections for scattering from single crystals in the absence of extinction should be evaluated using the Rayleigh cross section for a crystal in the non-reflecting position. However, as Rayleigh scattering is a minor contribution to the total absorption except for the lighter elements, no large error is made by applying the absorption correction appropriate to an assembly of isolated atoms to a single crystal.

Likewise, μ/ρ_m is, to a good approximation, given by the sum of the attenuation coefficients for each constituent element $(\mu/\rho_m)_a$, weighted by the mass fraction g_a for that element, *i.e.*

$$\frac{\mu}{\rho_m} = \sum_a g_a(\mu/\rho_m)_a, \qquad (6.3.1.5)$$

where the sum is over the elements. The atomic cross section for attenuation is given by

$$\sigma_a = (\mu/\rho_m)_a A_a/N_A = \mu/N_a, \qquad (6.3.1.6)$$

where A_a is the atomic weight and N_a is Avogadro's number. The evaluation of the attenuation coefficients is described in Section 4.2.4.

6.3.2. Dispersion

In the wavelength regime associated with anomalous scattering, where

$$f = f^0 + f' + f'', \qquad (6.3.2.1)$$

the refractive index becomes complex, its imaginary component contributing an additional term to the absorption.

f^0 is the scattering factor for ideal elastic scattering. The dispersion corrections f' and f'' are related to the absorption since (James, 1962; Wagenfeld, 1975)

$$f''(\omega) = mc\omega\sigma(\omega)/4\pi e^2, \quad \omega = 2\pi c/\lambda \qquad (6.3.2.2)$$

$$f'(\omega) = \frac{2}{\pi} \int_0^\infty [\omega' f''(\omega')/(\omega^2 - \omega'^2)]\, \mathrm{d}\omega'. \qquad (6.3.2.3)$$

That is, the dispersion corrections are determined by the absorption cross sections. The relationships (6.3.2.2) and (6.3.2.3) can be used in measuring absorption coefficients, as described in Section 4.2.4. The dispersion terms change rapidly near the absorption edge, especially on the short-wavelength side. The changes are anisotropic, sensitive to structure and to the direction of polarization. Details are given by Templeton & Templeton (1980, 1982, 1985).

In near-perfect crystals, the changes near the absorption edge are also sensitive to temperature (Karamura & Fukamachi, 1979; Fukamachi, Karamura, Hayakawa, Nakano & Koh, 1982). The effective absorption coefficient can also be altered by the Borrmann effect (Azaroff, Kaplow, Kato, Weiss, Wilson & Young, 1974).

6.3.3. Absorption corrections

The reduction in the intensity of an X-ray reflection from a uniform beam due to absorption is given by the transmission coefficient

$$A = \frac{1}{V} \int \exp(-\mu T)\, \mathrm{d}V, \qquad (6.3.3.1)$$

where the integration is over the volume of the crystal. The absorption correction

$$A^* = 1/A. \qquad (6.3.3.2)$$

T, the path length of the X-ray beam in the crystal, is the sum of the path lengths for the incident and diffracted beams. A technique for measuring crystals for absorption measurements is described in Subsection 6.3.3.6.

Any least-squares analysis involving variation of the linear absorption coefficient, or equivalently an isotropic variation in crystal size, requires the weighted mean path length

$$\bar{T} = -A^{-1} \frac{\partial A}{\partial \mu} = \frac{1}{A^*} \frac{\partial A^*}{\delta \mu}. \qquad (6.3.3.3)$$

This path length is also required in some analyses of extinction (Zachariasen, 1968; Becker & Coppens, 1974).

6.3.3.1. *Special cases*

For special cases, the integral can be solved analytically, and in some of these the expression reduces to closed form. These are listed in Table 6.3.3.1.

6.3.3.2. *Cylinders and spheres*

For diffraction in the equatorial plane of a cylinder of radius R within the X-ray beam, the expression for the transmission coefficient reduces to

$$A = \frac{1}{A^*} = \frac{1}{\pi R^2} \int_0^R \int_0^{2\pi} \exp\Big(- \mu\{[R^2 - r^2 \sin^2(\theta + \varphi)]^{1/2} + [R^2 - r^2 \sin^2(\theta - \varphi)]^{1/2}\}\Big) \times \cosh(2\mu r \sin\theta \sin\varphi) r\, \mathrm{d}r\, \mathrm{d}\varphi. \qquad (6.3.3.4)$$

Table 6.3.3.1. *Transmission coefficients*

(1) Reflection from a crystal slab with negligible transmission; the crystal planes are inclined at an angle φ to the extended face, and the normal in the plane of the incident and diffracted beams

$$A = \frac{\sin(\theta-\varphi)}{\mu\{\sin(\theta-\varphi)+\sin(\theta+\varphi)\}}$$

(1*a*) $\varphi = 0$

$$A = 1/2\mu$$

(2) Reflection from a crystal slab of thickness t, with planes parallel to the extended face

$$A = \{1-\exp(-2\mu t \operatorname{cosec}\theta)\}/2\mu$$

(3) Transmission through a crystal slab of thickness t; the crystal planes are at $\pi/2-\varphi$ to the surface, with the normal in the plane of the incident and reflected beams

$$A = \frac{\exp\{-\mu t\sec(\theta+\varphi)\}-\exp\{-\mu t\sec(\theta-\varphi)\}}{\mu\left[1-\dfrac{\sec(\theta+\varphi)}{\sec(\theta-\varphi)}\right]}$$

(3*a*) $\varphi = 0$

$$A = t\sec\theta\exp(-\mu t\sec\theta)$$

(4) Transmission through a sphere of radius R (*i.e.* for a uniform X-ray beam and $\theta = 0^\circ$)

$$A = \frac{3}{2(\mu R)^3}[1/2 - e^{-2\mu R}\{1/2+\mu R+(\mu R)^2\}]$$

(5) Reflection from a sphere of radius R (*i.e.* for a uniform X-ray beam, and $\theta = 90^\circ$)

$$A = \frac{3}{4\mu R}\left\{1/2 - \frac{1}{16(\mu R)^2}\,[1-(1+4\mu R)\,e^{-4\mu R}]\right\}$$

Values of the absorption correction A^* obtained by numerical integration by Dwiggins (1975*a*) are listed in Table 6.3.3.2.

The reduced expression for a spherical crystal of radius R is

$$\begin{aligned}A = \frac{3}{4\pi R^3}\int_0^R\int_{-1}^1\int_0^{2\pi} \exp\Big(-\mu\{&[R^2 - r^2\cos^2\alpha \\ &- r^2\sin^2\alpha\sin^2(\theta+\varphi)]^{1/2} \\ &+ [R^2 - r^2\cos^2\alpha - r^2\sin^2\alpha\sin^2(\theta-\varphi)]^{1/2} \\ &- 2r\sin\theta\sin\alpha\sin\varphi\}\Big) r^2\,\mathrm{d}r\,\mathrm{d}(\cos\alpha)\,\mathrm{d}\varphi. \qquad (6.3.3.5)\end{aligned}$$

Values of A^* obtained using numerical integration by Dwiggins (1975*b*) are listed in Table 6.3.3.3. An estimate of the accuracy of the numerical integration is given by comparison with the results for special values of θ at which equations (6.3.3.4) and (6.3.3.5) may be integrated analytically, which are included in Table 6.3.3.1. The comparison indicates a reliability for the tabulated values of better than 0.1%. Tables at finer intervals for cylinders and spheres for $\mu R < 1.0$ are given by Rouse, Cooper, York & Chakera (1970). A tabulation up to $\mu R < 5.0$ for spheres is given by Weber (1969). Interpolation for μR may be effected by the formula

$$A^*(\mu R) = \exp\left\{\sum_{m=1}^{M} K_m(\mu R)^m\right\}, \qquad (6.3.3.6)$$

where the K_m are determined, for fixed θ, from the values in Tables 6.3.3.2 and 6.3.3.3.

Subsequent interpolation as a function of θ may be effected by the interpolation formula

$$A^*\{\theta\} = \sum_{n=1}^{N} L_n \sin^{2n}(\theta). \qquad (6.3.3.7)$$

Interpolation is accurate to 0.1% with $N = M = 3$.

For cylinders and spheres, $\bar{T}$ may be obtained by means of the expression

$$\bar{T} = \frac{1}{A^*}\frac{\mathrm{d}A^*}{\mathrm{d}\mu} = R\left[\frac{1}{A^*}\frac{\mathrm{d}A^*}{\mathrm{d}(\mu R)}\right] \qquad (6.3.3.8)$$

using the values listed in Tables 6.3.3.2 and 6.3.3.3.

Values of $(1/A^*)[\mathrm{d}A^*/\mathrm{d}(\mu R)]$ obtained by numerical integration by Flack & Vincent (1978) for spheres with $\mu R < 2.5$ are listed in Table 6.3.3.4. An equivalent table of $\mu(R/A^*)/[\mathrm{d}A^*/\mathrm{d}(\mu R)]$ for $\mu R < 4.0$ is given by Rigoult & Guidi-Morosini (1980).

Alternatively, one can differentiate the interpolation formula (6.3.3.6), yielding

$$\bar{T}(\mu R,\theta) = \frac{1}{\mu}\sum_{m=1}^{M} mK_m(\mu R)^m. \qquad (6.3.3.9)$$

In this case, however, the maximum index $M = 7$ is required to obtain convergence for $\mu R \le 2.5$. Numerical values of the coefficients K_m for cylinders and spheres evaluated by Tibballs (1982) are listed in Table 6.3.3.5.

Interpolation between the tabulated θ values is obtained from the θ interpolation formula, noting that

$$L_m = \sum_{j=1}^{7} (C^{-1})_{mj} A_j^*, \qquad (6.3.3.10)$$

where

$$C_{mj} = \sin^{2m}\theta_j. \qquad (6.3.3.11)$$

The elements $(C^{-1})_{mj}$ and the $K_m(\theta_j)$ for θ_j at 15° intervals in the range $0 < \theta_j < 90^\circ$ are listed in Table 6.3.3.5. Differentiating (6.3.3.7) yields

$$A^*(\mu R,\theta)\bar{T}(\mu R,\theta) = \sum_{m=0}^{M} P_m \sin^{2m}\theta, \qquad (6.3.3.12)$$

where

$$P_m = R\frac{\partial L_m}{\partial(\mu R)} = \sum_{j=1}^{7}(C^{-1})_{mj}A_j^*\bar{T}_j. \qquad (6.3.3.13)$$

Equation (6.3.3.12) for path lengths is the analogue of equation (6.3.3.7) for the transmission factors. It provides the basis for an interpolation formula.

In the case of a cylindrical crystal much larger than the X-ray beam, the absorption correction has been determined by Coyle (1972), in an extension of earlier work by Coyle & Schroeder (1971). The absorption correction for the case of the cylinder axis coincident with the φ axis of a Eulerian cradle, shown in Fig. 6.3.3.1, reduces to the line integral

$$\frac{1}{2\tau}\int_0^{2\tau} \exp\{-\mu[(z)+T(z)]\}\,\mathrm{d}z, \qquad (6.3.3.14)$$

Table 6.3.3.2. *Values of A^* for cylinders*

μR	$\theta = 0°$	$\theta = 5°$	$\theta = 10°$	$\theta = 15°$	$\theta = 20°$	$\theta = 25°$	$\theta = 30°$	$\theta = 35°$	$\theta = 40°$	$\theta = 45°$	$\theta = 50°$	$\theta = 55°$	$\theta = 60°$	$\theta = 65°$	$\theta = 70°$	$\theta = 75°$	$\theta = 80°$	$\theta = 85°$	$\theta = 90°$
0.0	1	1	1	1	1	1	1	1	1	1	1	1	1	1	1	1	1	1	1
0.1	1.1843	1.1843	1.1842	1.1840	1.1838	1.1835	1.1832	1.1828	1.1823	1.1818	1.1813	1.1808	1.1802	1.1798	1.1793	1.1790	1.1787	1.1785	1.1785
0.2	1.4009	1.4007	1.4002	1.3995	1.3984	1.3970	1.3953	1.3934	1.3912	1.3889	1.3865	1.3841	1.3818	1.3796	1.3777	1.3761	1.3749	1.3741	1.3739
0.3	1.6548	1.6544	1.6531	1.6510	1.6481	1.6443	1.6398	1.6347	1.6290	1.6230	1.6169	1.6108	1.6049	1.5994	1.5946	1.5906	1.5876	1.5857	1.5851
0.4	1.9522	1.9513	1.9485	1.9439	1.9376	1.9296	1.9201	1.9094	1.8979	1.8857	1.8733	1.8611	1.8495	1.8388	1.8293	1.8215	1.8157	1.8121	1.8108
0.5	2.2996	2.2979	2.2926	2.2840	2.2721	2.2572	2.2398	2.2204	2.1996	2.1781	2.1564	2.1352	2.1152	2.0969	2.0809	2.0677	2.0579	2.0518	2.0497
0.6	2.7047	2.7017	2.6926	2.6775	2.6570	2.6317	2.6023	2.5701	2.5359	2.5010	2.4662	2.4327	2.4012	2.3728	2.3480	2.3277	2.3126	2.3033	2.3001
0.7	3.1762	3.1712	3.1561	3.1315	3.0982	3.0575	3.0111	2.9607	2.9081	2.8549	2.8028	2.7530	2.7068	2.6653	2.6295	2.6003	2.5786	2.5651	2.5606
0.8	3.7236	3.7157	3.6919	3.6532	3.6015	3.5392	3.4691	3.3941	3.3169	3.2400	3.1656	3.0953	3.0307	2.9732	2.9239	2.8839	2.8542	2.8359	2.8297
0.9	4.3578	4.3456	4.3093	4.2507	4.1733	4.0812	3.9792	3.8718	3.7629	3.6560	3.5538	3.4584	3.3717	3.2951	3.2299	3.1772	3.1383	3.1142	3.1061
1.0	5.0907	5.0724	5.0185	4.9323	4.8196	4.6877	4.5439	4.3948	4.2461	4.1022	3.9664	3.8413	3.7286	3.6298	3.5462	3.4790	3.4295	3.3990	3.3886
1.1	5.9356	5.9089	5.8305	5.7065	5.5466	5.3624	5.1649	4.9636	4.7660	4.5776	4.4022	4.2424	4.0998	3.9759	3.8717	3.7882	3.7269	3.6891	3.6763
1.2	6.907	6.869	6.757	6.582	6.360	6.109	5.8436	5.5782	5.3219	5.0811	4.8598	4.6604	4.4842	4.3322	4.2051	4.1038	4.0295	3.9838	3.9682
1.3	8.021	7.967	7.810	7.568	7.266	6.929	6.581	6.238	5.9125	5.6110	5.3376	5.0938	4.8805	4.6976	4.5456	4.4248	4.3365	4.2821	4.2636
1.4	9.294	9.219	9.003	8.674	8.268	7.826	7.376	6.942	6.536	6.166	5.8341	5.5413	5.2873	5.0711	4.8922	4.7506	4.6471	4.5835	4.5619
1.5	10.746	10.643	10.349	9.907	9.372	8.800	8.230	7.689	7.192	6.744	6.348	6.002	5.7036	5.4516	5.2441	5.0804	4.9609	4.8875	4.8625
1.6	12.397	12.257	11.862	11.276	10.581	9.852	9.141	8.477	7.877	7.344	6.877	6.473	6.128	5.8385	5.6007	5.4136	5.2773	5.1935	5.1650
1.7	14.267	14.080	13.555	12.788	11.897	10.982	10.106	9.304	8.589	7.963	7.420	6.955	6.561	6.231	5.961	5.7499	5.5960	5.5014	5.4691
1.8	16.379	16.131	15.441	14.450	13.323	12.189	11.125	10.168	9.327	8.600	7.976	7.446	7.000	6.628	6.326	6.089	5.9166	5.8107	5.7746
1.9	18.76	18.43	17.53	16.267	14.858	13.470	12.194	11.066	10.089	9.253	8.544	7.946	7.444	7.030	6.693	6.430	6.239	6.121	6.081
2.0	21.43	21.00	19.84	18.24	16.50	14.824	13.311	11.995	10.871	9.921	9.122	8.452	7.895	7.435	7.063	6.773	6.562	6.433	6.389
2.1	24.41	23.87	22.39	20.38	18.25	16.247	14.472	12.953	11.673	10.602	9.709	8.965	8.349	7.843	7.436	7.118	6.887	6.745	6.697
2.2	27.74	27.04	25.17	22.69	20.11	17.74	15.675	13.938	12.493	11.295	10.304	9.484	8.808	8.255	7.810	7.464	7.213	7.059	7.006
2.3	31.44	30.55	28.20	25.16	22.07	19.29	16.92	14.947	13.328	11.999	10.906	10.008	9.271	8.669	8.187	7.812	7.540	7.372	7.315
2.4	35.54	34.41	31.49	27.79	24.13	20.90	18.19	15.978	14.177	12.711	11.515	10.537	9.736	9.086	8.565	8.161	7.868	7.687	7.625
2.5	40.06	38.65	35.05	30.59	26.28	22.56	19.50	17.03	15.040	13.433	12.130	11.069	10.205	9.505	8.945	8.511	8.196	8.002	7.935

Table 6.3.3.3. *Values of A^* for spheres*

μR	$\theta = 0°$	$\theta = 5°$	$\theta = 10°$	$\theta = 15°$	$\theta = 20°$	$\theta = 25°$	$\theta = 30°$	$\theta = 35°$	$\theta = 40°$	$\theta = 45°$	$\theta = 50°$	$\theta = 55°$	$\theta = 60°$	$\theta = 65°$	$\theta = 70°$	$\theta = 75°$	$\theta = 80°$	$\theta = 85°$	$\theta = 90°$
0.0	1	1	1	1	1	1	1	1	1	1	1	1	1	1	1	1	1	1	1
0.1	1.1609	1.1609	1.1609	1.1607	1.1606	1.1603	1.1600	1.1597	1.1593	1.1589	1.1586	1.1582	1.1579	1.1575	1.1572	1.1570	1.1568	1.1567	1.1567
0.2	1.3457	1.3456	1.3452	1.3447	1.3439	1.3428	1.3415	1.3400	1.3383	1.3366	1.3348	1.3331	1.3313	1.3297	1.3282	1.3271	1.3262	1.3256	1.3254
0.3	1.5574	1.5571	1.5561	1.5546	1.5525	1.5497	1.5463	1.5426	1.5383	1.5339	1.5293	1.5248	1.5204	1.5162	1.5126	1.5096	1.5074	1.5059	1.5055
0.4	1.7994	1.7988	1.7968	1.7935	1.7891	1.7833	1.7765	1.7689	1.7604	1.7515	1.7425	1.7335	1.7249	1.7169	1.7099	1.7041	1.6997	1.6970	1.6961
0.5	2.0755	2.0743	2.0706	2.0647	2.0565	2.0462	2.0340	2.0204	2.0056	1.9901	1.9745	1.9592	1.9445	1.9311	1.9194	1.9097	1.9024	1.8979	1.8964
0.6	2.3897	2.3877	2.3816	2.3715	2.3578	2.3406	2.3206	2.2984	2.2746	2.2500	2.2255	2.2015	2.1789	2.1583	2.1403	2.1257	2.1145	2.1076	2.1063
0.7	2.7467	2.7434	2.7336	2.7177	2.6959	2.6691	2.6382	2.6042	2.5683	2.5316	2.4952	2.4602	2.4274	2.3977	2.3719	2.3508	2.3351	2.3253	2.3220
0.8	3.1511	3.1461	3.1312	3.1069	3.0740	3.0339	2.9882	2.9386	2.8869	2.8347	2.7835	2.7346	2.6892	2.6484	2.6133	2.5845	2.5632	2.5499	2.5454
0.9	3.6082	3.6009	3.5789	3.5431	3.4952	3.4374	3.3723	3.3026	3.2308	3.1592	3.0898	3.0241	2.9637	2.9098	2.8634	2.8258	2.7979	2.7805	2.7747
1.0	4.1237	4.1131	4.0815	4.0304	3.9625	3.8816	3.7917	3.6966	3.6001	3.5048	3.4135	3.3280	3.2499	3.1807	3.1216	3.0738	3.0383	3.0163	3.0090
1.1	4.7035	4.6886	4.6442	4.5729	4.4790	4.3686	4.2474	4.1211	3.9945	3.8710	3.7540	3.6455	3.5470	3.4605	3.3870	3.3276	3.2838	3.2566	3.2474
1.2	5.3542	5.3335	5.2722	5.1747	5.0476	4.9001	4.7404	4.5761	4.4137	4.2571	4.1104	3.9756	3.8542	3.7483	3.6586	3.5866	3.5334	3.5005	3.4894
1.3	6.082	6.054	5.9710	5.8399	5.6710	5.4776	5.2711	5.0617	4.8573	4.6625	4.4819	4.3175	4.1706	4.0432	3.9360	3.8500	3.7868	3.7477	3.7344
1.4	6.895	6.857	6.746	6.573	6.352	6.102	5.8400	5.5774	5.3244	5.0862	4.8676	4.6703	4.4955	4.3447	4.2183	4.1174	4.0432	3.9974	3.9819
1.5	7.801	7.750	7.604	7.377	7.092	6.775	6.447	6.123	5.8143	5.5273	5.2666	5.0333	4.8281	4.6520	4.5052	4.3883	4.3024	4.2495	4.2315
1.6	8.806	8.740	8.549	8.256	7.894	7.497	7.092	6.697	6.326	5.9849	5.6780	5.4057	5.1678	4.9647	4.7961	4.6622	4.5641	4.5036	4.4830
1.7	9.920	9.834	9.587	9.214	8.759	8.268	7.774	7.299	6.859	6.458	6.101	5.7867	5.5140	5.2823	5.0907	4.9390	4.8279	4.7595	4.7361
1.8	11.151	11.040	10.725	10.254	9.689	9.088	8.492	7.928	7.411	6.946	6.535	6.176	5.8662	5.6045	5.3888	5.2184	5.0936	5.0170	4.9908
1.9	12.507	12.366	11.967	11.380	10.685	9.957	9.246	8.583	7.982	7.447	6.978	6.572	6.224	5.9308	5.6900	5.5001	5.3613	5.2760	5.2468
2.0	13.998	13.819	13.320	12.593	11.746	10.873	10.034	9.262	8.570	7.961	7.431	6.975	6.587	6.261	5.9942	5.7842	5.6307	5.5365	5.5041
2.1	15.632	15.408	14.788	13.895	12.874	11.837	10.855	9.964	9.175	8.486	7.893	7.385	6.955	6.595	6.301	6.070	5.9017	5.7982	5.7627
2.2	17.419	17.141	16.376	15.290	14.067	12.847	11.708	10.688	9.795	9.023	8.362	7.800	7.327	6.932	6.610	6.358	6.174	6.061	6.022
2.3	19.369	19.025	18.089	16.778	15.327	13.902	12.592	11.433	10.429	9.569	8.839	8.220	7.702	7.272	6.922	6.648	6.448	6.325	6.282
2.4	21.489	21.069	19.931	18.361	16.652	15.000	13.504	12.198	11.077	10.125	9.322	8.645	8.081	7.614	7.235	6.938	6.722	6.589	6.543
2.5	23.791	23.280	21.907	20.040	18.041	16.142	14.445	12.982	11.738	10.690	9.810	9.074	8.462	7.957	7.548	7.229	6.996	6.853	6.803

Table 6.3.3.4. *Values of* $(1/A^*)(dA^*/d\mu R)$ *for spheres*

μR	$\theta = 0°$	$\theta = 5°$	$\theta = 10°$	$\theta = 15°$	$\theta = 20°$	$\theta = 25°$	$\theta = 30°$	$\theta = 35°$	$\theta = 40°$	$\theta = 45°$	$\theta = 50°$	$\theta = 55°$	$\theta = 60°$	$\theta = 65°$	$\theta = 70°$	$\theta = 75°$	$\theta = 80°$	$\theta = 85°$	$\theta = 90°$
0.0	1.5000	1.5000	1.5000	1.5000	1.5000	1.5000	1.5000	1.5000	1.5000	1.5000	1.5000	1.5000	1.5000	1.5000	1.5000	1.5000	1.5000	1.5000	1.5000
0.1	1.4845	1.4842	1.4829	1.4809	1.4782	1.4739	1.4690	1.4634	1.4569	1.4504	1.4439	1.4375	1.4309	1.4248	1.4191	1.4152	1.4117	1.4096	1.4089
0.2	1.4692	1.4682	1.4650	1.4611	1.4548	1.4472	1.4374	1.4268	1.4145	1.4019	1.3879	1.3748	1.3615	1.3491	1.3385	1.3292	1.3228	1.3180	1.3168
0.3	1.4527	1.4515	1.4476	1.4400	1.4309	1.4186	1.4044	1.3886	1.3708	1.3517	1.3327	1.3128	1.2947	1.2773	1.2624	1.2494	1.2397	1.2340	1.2321
0.4	1.4360	1.4341	1.4283	1.4190	1.4058	1.3898	1.3709	1.3492	1.3265	1.3018	1.2773	1.2531	1.2296	1.2089	1.1903	1.1748	1.1628	1.1560	1.1533
0.5	1.4186	1.4161	1.4090	1.3969	1.3803	1.3598	1.3360	1.3093	1.2812	1.2522	1.2231	1.1946	1.1678	1.1434	1.1218	1.1044	1.0910	1.0825	1.0797
0.6	1.4011	1.3980	1.3890	1.3742	1.3538	1.3289	1.3006	1.2693	1.2365	1.2033	1.1700	1.1382	1.1087	1.0816	1.0577	1.0383	1.0239	1.0147	1.0115
0.7	1.3830	1.3792	1.3683	1.3507	1.3264	1.2973	1.2643	1.2286	1.1918	1.1549	1.1184	1.0839	1.0516	1.0250	0.9978	0.9767	0.9615	0.9518	0.9484
0.8	1.3641	1.3600	1.3473	1.3262	1.2984	1.2650	1.2275	1.1879	1.1473	1.1071	1.0684	1.0314	0.9976	0.9674	0.9409	0.9195	0.9034	0.8931	0.8898
0.9	1.3451	1.3401	1.3253	1.3013	1.2696	1.2321	1.1908	1.1474	1.1038	1.0608	1.0198	0.9815	0.9465	0.9152	0.8880	0.8663	0.8495	0.8391	0.8359
1.0	1.3255	1.3198	1.3029	1.2758	1.2401	1.1987	1.1535	1.1070	1.0608	1.0157	0.9733	0.9340	0.8978	0.8661	0.8392	0.8167	0.8001	0.7897	0.7859
1.1	1.3058	1.2993	1.2800	1.2497	1.2103	1.1651	1.1165	1.0670	1.0185	0.9720	0.9286	0.8886	0.8522	0.8205	0.7931	0.7709	0.7542	0.7437	0.7400
1.2	1.2851	1.2780	1.2566	1.2228	1.1799	1.1312	1.0796	1.0278	0.9777	0.9299	0.8858	0.8455	0.8093	0.7776	0.7506	0.7285	0.7120	0.7017	0.6981
1.3	1.2645	1.2563	1.2324	1.1961	1.1494	1.0967	1.0430	0.9892	0.9377	0.8895	0.8451	0.8048	0.7691	0.7378	0.7113	0.6895	0.6733	0.6631	0.6596
1.4	1.2449	1.2349	1.2090	1.1684	1.1180	1.0628	1.0068	0.9517	0.8990	0.8504	0.8064	0.7666	0.7315	0.7009	0.6749	0.6539	0.6377	0.6278	0.6243
1.5	1.2231	1.2133	1.1845	1.1398	1.0867	1.0295	0.9711	0.9145	0.8615	0.8133	0.7696	0.7308	0.6964	0.6665	0.6414	0.6209	0.6055	0.5957	0.5922
1.6	1.2015	1.1908	1.1585	1.1118	1.0555	0.9957	0.9358	0.8782	0.8261	0.7778	0.7350	0.6970	0.6638	0.6349	0.6105	0.5907	0.5758	0.5663	0.5628
1.7	1.1806	1.1681	1.1339	1.0836	1.0244	0.9621	0.9005	0.8435	0.7912	0.7444	0.7027	0.6659	0.6334	0.6057	0.5822	0.5632	0.5484	0.5394	0.5361
1.8	1.1586	1.1456	1.1087	1.0558	0.9939	0.9294	0.8669	0.8101	0.7579	0.7121	0.6711	0.6359	0.6053	0.5787	0.5561	0.5376	0.5236	0.5148	0.5117
1.9	1.1370	1.1226	1.0835	1.0275	0.9625	0.8964	0.8341	0.7774	0.7262	0.6817	0.6420	0.6078	0.5791	0.5535	0.5321	0.5144	0.5010	0.4924	0.4892
2.0	1.1152	1.0996	1.0584	0.9982	0.9318	0.8646	0.8019	0.7457	0.6962	0.6527	0.6160	0.5830	0.5550	0.5305	0.5098	0.4927	0.4799	0.4717	0.4687
2.1	1.0932	1.0772	1.0327	0.9703	0.9014	0.8340	0.7712	0.7157	0.6678	0.6259	0.5899	0.5588	0.5322	0.5088	0.4886	0.4726	0.4603	0.4523	0.4494
2.2	1.0719	1.0543	1.0074	0.9427	0.8719	0.8039	0.7421	0.6874	0.6402	0.6003	0.5658	0.5353	0.5098	0.4884	0.4699	0.4548	0.4426	0.4347	0.4311
2.3	1.0498	1.0316	0.9822	0.9150	0.8434	0.7744	0.7133	0.6605	0.6147	0.5758	0.5433	0.5141	0.4896	0.4692	0.4518	0.4363	0.4252	0.4175	0.4149
2.4	1.0275	1.0118	0.9583	0.8889	0.8147	0.7482	0.6870	0.6340	0.5918	0.5507	0.5212	0.4937	0.4699	0.4500	0.4328	0.4187	0.4076	0.4003	0.3986
2.5	1.0108	0.9691	0.9297	0.8562	0.7904	0.7074	0.6554	0.6194	0.5618	0.5289	0.4980	0.4776	0.4554	0.4315	0.4142	0.4028	0.3921	0.3883	0.3783

Table 6.3.3.5. *Coefficients for interpolation of* A^* *and* $\bar{T}$

θ_j	0°	15°	30°	45°	60°	75°	90°	Units
K_1 (sphere)	3/2	3/2	3/2	3/2	3/2	3/2	3/2	
K_2	−7.5234	−9.4320	−15.109	−24.3812	−35.219	−44.042	−47.745	10^{-2}
K_3	−7.0935	−10.737	−18.027	−11.088	14.265	40.021	61.084	10^{-3}
K_4	−2.3096	−2.1332	−1.4693	7.4205	24.832	44.308	37.394	10^{-3}
K_5	1.8323	1.1711	4.6784	3.0970	−10.284	−27.987	−25.879	10^{-3}
K_6	−5.1259	−1.2652	−14.491	−16.740	21.910	77.007	71.458	10^{-4}
K_7	6.0265	0.7932	16.489	21.774	−22.391	−85.570	−78.812	10^{-5}
K_1 (cylinder)	$16/3\pi$	$16/3\pi$	$16/3\pi$	$16/3\pi$	$16/3\pi$	$16/3\pi$	$16/3\pi$	
K_2	−5.7832	−8.1900	−15.651	−27.048	−40.317	−51.497	−55.837	10^{-2}
K_3	−14.737	−19.551	−22.883	−27.345	−8.807	26.637	41.420	10^{-3}
K_4	5.2399	1.2934	−12.301	6.844	40.689	61.371	68.963	10^{-3}
K_5	−4.0958	−2.8349	9.6249	7.503	−11.295	−29.397	−36.556	10^{-3}
K_6	13.178	12.731	−19.881	−30.211	9.4468	60.356	80.965	10^{-4}
K_7	−14.500	−14.846	14.414	34.222	3.1492	−49.206	−70.573	10^{-5}
$(C^{-1})_{0j}$	3	0	0	0	0	0	0	All values
$(C^{-1})_{1j}$	−73	$48+24\sqrt{3}$	−24	12	−8	$48-24\sqrt{3}$	−3	multiplied
$(C^{-1})_{2j}$	518	$-496-200\sqrt{3}$	488	−268	184	$-496+200\sqrt{3}$	70	by 3
$(C^{-1})_{3j}$	−1600	$1920+560\sqrt{3}$	−2192	1536	−1136	$1920-560\sqrt{3}$	−448	to eliminate
$(C^{-1})_{4j}$	2432	$-3520-640\sqrt{3}$	4032	−3328	2752	$-3520+640\sqrt{3}$	1152	fractions
$(C^{-1})_{5j}$	−1792	$3072+256\sqrt{3}$	−3328	3072	−2816	$3072-256\sqrt{3}$	−1280	
$(C^{-1})_{6j}$	512	−1024	1024	−1024	1024	−1024	512	

where z and $T(z)$ are the path lengths for the incident and diffracted beams, respectively. τ is the radius, along the line of the incident beam, of the ellipse described by the cross section of the crystal in the plane of diffraction, shown in Fig. 6.3.3.2. The equation for the ellipse is

$$\tau = R(1 - \sin^2\theta \sin^2\chi)^{-1/2}. \qquad (6.3.3.15)$$

The outgoing elliptical radius v satisfies

$$Av^4 + Bv^2 + C = 0, \qquad (6.3.3.16)$$

where

$$\begin{aligned} A &= [1 - \sin^2\theta \sin^2\chi]^2 \\ B &= -2R^2[1 - \sin^2\theta \sin^2\chi] \\ &\quad - 2(\tau - z)^2[\cos^2\theta - \sin^2\theta \cos^2\chi] \sin^2 2\theta \sin^2\chi \\ C &= R^4 + 2R^2(\tau - z)^2 \sin^2 2\theta \sin^2\chi \cos 2\theta \\ &\quad + (\tau - z)^4 \sin^4 2\theta \sin^4\chi. \end{aligned}$$

In the case where the cylinder axis is inclined at an angle Γ to the φ axis, these equations become

$$\begin{aligned} A &= [1 - \sin^2(\theta + \beta) \sin^2\chi_1]^2 \\ B &= -2R^2[1 - \sin^2(\theta + \beta) \sin^2\chi_1] \\ &\quad - 2(\tau - z)^2[\cos^2(\theta + \beta) \\ &\quad - \sin^2(\theta + \beta) \cos^2\chi_1] \sin^2 2\theta \sin^2\chi_1 \\ C &= R^4 + 2R^2(\tau - z)^2 \sin^2 2\theta \sin^2\chi_1 \cos 2(\theta + \beta) \\ &\quad + (\tau - z)^4 \sin^4 2\theta \sin^4\chi_1, \end{aligned}$$

where

$$\tan\beta = \sin\Gamma \sin\varphi / [\sin\Gamma \cos\chi \cos\varphi + \sin\chi \cos\Gamma].$$

The roots of the quadratic equation (6.3.3.16) for v^2 are real and positive for reflection from within the crystal. The convergent path length T is given by the positive root of the triangle formula

$$T^2 - 2T(\tau - z)\cos 2\theta + (\tau - z)^2 - v^2 = 0. \qquad (6.3.3.17)$$

It should be noted that the volume of the specimen irradiated changes with the angular settings of the diffractometer. Normalization to constant volume requires that the absorption correction be multiplied by the volume-correction factor $[1 - \sin^2(\theta - \beta)\sin^2\chi_1]^{-1/2}$.

The method readily extends to the case of a cylindrical window or sheath, such as used for mounting an unstable crystal of conventional size. The correction in this case is

$$\begin{aligned} &\exp[-\mu(\tau_2 - \tau_1 + v_2 - v_1)] \\ &\quad = \exp\Big(- \mu(R_2 - R_1)\{[1 - \sin^2(\theta - \beta)\sin^2\chi_1]^{-1/2} \\ &\qquad + [1 - \sin^2(\theta + \beta)\sin^2\chi_1]^{-1/2}\}\Big), \end{aligned} \qquad (6.3.3.18)$$

where the subscripts 1 and 2 apply to the inner and outer radii, respectively.

The integral in equation (6.3.3.14) may be evaluated by Gaussian quadrature, *i.e.* by approximation as a weighted sum of the values of the function at the N zeros X_i of the Legendre polynomial of degree N in the interval $[-1, +1]$. The weights w_i for the points are tabulated by Abramowitz & Stegun (1964). Further details are given in Subsection 6.3.3.4. The emergent path lengths $T(z_1)$ and $T(z_2)$ for the case of the sheath are calculated as functions of the Gaussian variable X_i using the linear transformation

$$z_i = \tau_1 X_i + \tau_2, \quad i = 1, 2, \ldots, N. \qquad (6.3.3.19)$$

This transformation converts the Gaussian variable X into the beam coordinate z for each i of the N summation points.

6.3.3.3. *Analytical method for crystals with regular faces*

For a crystal with regular faces, (6.3.3.1) may be integrated exactly, giving the correction in analytical form. In its simplest form, the analytical method applies to specimens with no re-entrant angles. It is efficient for crystals with a small number of faces. Its accuracy does not depend on the size of the absorption coefficient. The principles can be illustrated by reference to the two-dimensional case of a triangular crystal shown in Fig. 6.3.3.3.

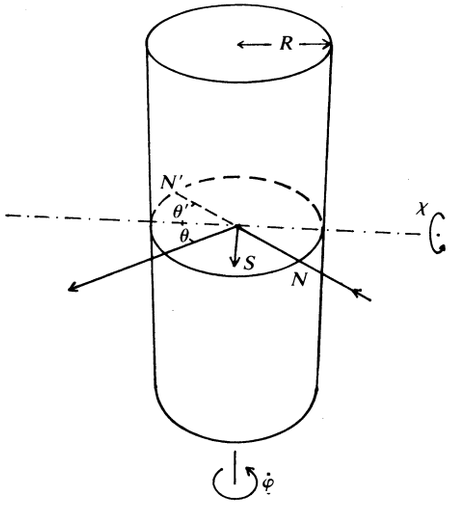

Fig. 6.3.3.1. Geometry of the Eulerian cradle with the axis of a cylindrical specimen coincident with the φ axis.

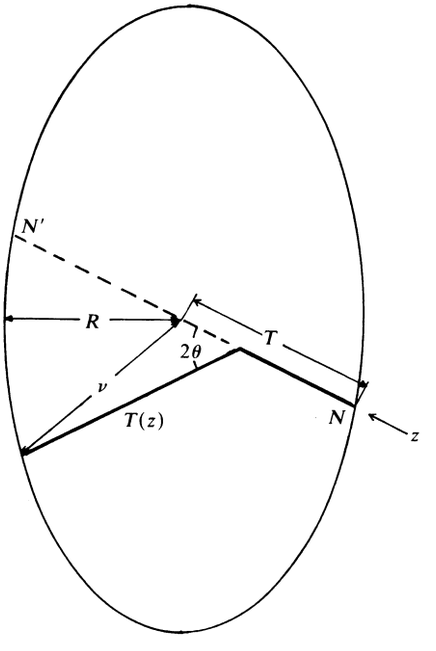

Fig. 6.3.3.2. Cross section of the plane of diffraction for a cylindrical specimen coincident with the φ axis.

The crystal is divided into polygons *ADC*, *AFD*, *CDE*, and *BEDF* as shown. The radiation incident on each polygon enters through one face of the crystal, and is either absorbed or emerges through another. Within each polygon, the loci of constant absorption are the straight lines dotted in Fig. 6.3.3.3. It is convenient to subdivide *BEDF* into the triangles *BEF* and *EDF*. By the derivation of an expression for the contribution of a triangular crystal to the scattering, including allowance for absorption, and with the sum taken over the component triangles *ADC*, *AFD*, *CDE*, *BEF*, and *EDF*, the correction for absorption can be calculated.

A three-dimensional crystal is divided into polyhedra, for each of which the radiation enters through one crystal face and leaves through another. Corners for the polyhedra are of five types, namely,

(1) Crystal vertex.

(2) An intersection of a ray through a lit vertex with an opposite face.

(3) An intersection of an incident ray through a lit (*i*) vertex with a plane of diffracted (*d*) rays through a lit (*d*) edge, and the corresponding intersection with incident and diffracted beams interchanged.

(4) An intersection of a plane of incident rays through a lit (*i*) edge with an opposite edge, and its equivalent.

(5) An intersection on a shaded face of planes of incident and diffracted rays through (*i*) and (*d*) edges.

For each vertex x, y, z, the sum of the path lengths to each of the crystal faces is calculated, and multiplied by the absorption coefficient μ to give the optical path length using the equation

$$\mu r_j = \mu(d_j - a_j x - b_j y - c_j z)/(a_j u + b_j v + c_j w),$$

where u, v, w are the direction cosines for the beam direction, and $a_j x + b_j y + c_j z = d_j$ is the equation for the crystal face. The minimum for all j is the path length to the surface.

The analytical expression for the scattering power for each polyhedron, including the effect of absorption, can be expressed in a convenient form by subdividing the polyhedra into tetrahedra. The auxiliary points define the corners of the tetrahedra.

The total diffracted intensity is proportional to the sum of contributions, one from each tetrahedron, of the form

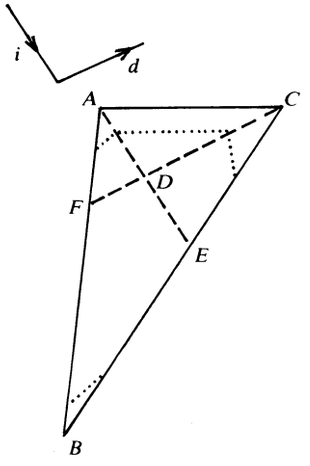

Fig. 6.3.3.3. The crystal *ABC* divided into polygons by the dashed lines *AE* and *CF* parallel to the incident (*i*) and diffracted (*d*) beams, respectively. A locus of constant absorption is shown dotted.

$$R_t = 6V_t e^{-g} H(1)$$
$$= \frac{6V_t}{(b+c)} e^{-g}\left\{\frac{h(a)-h(a+b)}{b} - \frac{h(a+b)-h(a+b+c)}{c}\right\}, \tag{6.3.3.20}$$

where

$$h(x) = \frac{1-e^{-x}}{x}. \tag{6.3.3.21}$$

V_t is the volume of the tetrahedron. For a crystal with Cartesian coordinate vertices 1, 2, 3, and 4,

$$V_t = \tfrac{1}{6}\begin{vmatrix} x_1-x_2 & x_1-x_3 & x_1-x_4 \\ y_1-y_2 & y_1-y_3 & y_1-y_4 \\ z_1-z_2 & z_1-z_3 & z_1-z_4 \end{vmatrix}. \tag{6.3.3.22}$$

The g_i are optical path lengths (*i.e.* path lengths rescaled by the absorption coefficient) ordered so that

$$g_1 < g_2 < g_3 < g_4$$

and

$$g = g_1, \quad a = g_2 - g_1, \quad b = g_3 - g_2, \quad c = g_4 - g_3. \tag{6.3.3.23}$$

The transmission factor for the crystal is the sum of the scattering powers for all the tetrahedra $\sum R_t$ divided by the volume $\sum V_t$. The equality of the total volume to the sum of the V_t values for the component tetrahedra provides a useful check on the accuracy of the calculations, since the total volume is independent of the beam directions, and must be the same for all reflections.

When any of a, b, and c are small, asymptotic forms are required for the expressions in (6.3.3.20). For $\varepsilon < 0.3 \times 10^{-2}$, and

$a < \varepsilon$ $\quad h(a) = 1 - a/2 + a^2/3!$
$\quad h(b+a) = h(b) + ah_1(b) + a^2 h_2(b)/2;$

$b < \varepsilon$ $\quad h(a+b) = h(a) + bh_1(a) + b^2 h_2(a)/2$
$\quad [h(a) - h(a+b)]/b$
$\quad = -h_1(a) - bh_2(a)/2 - b^2 h_3(a)/3!;$

$c < \varepsilon$ $\quad [h(a+b) - h(a+b+c)]/c$
$\quad = -h_1(a+b) - ch_2(a+b)/2$
$\quad -c^2 h_3(a+b)/3!;$

$b, c < \varepsilon$ $\quad H(1) = h_2(a)/2 + (2b+c)h_3(a)/3!$
$\quad + (3b^2 + 3bc + c^2)h_4(a)/4!;$

$a, c < \varepsilon$ $\quad h(a) = 1 - a/2 + a^2/3!$
$\quad [h(a+b) - h(a+b+c)]/c$
$\quad = -h_1(a+b) - ch_2(a+b)/2$
$\quad -c^2 h_3(a+b)/3!;$

$a, b < \varepsilon$ $\quad h(a+b) = 1 - (a+b)/2 + (a+b)^2/3!$
$\quad [h(a) - h(a+b)]/b$
$\quad = 1/2 - a/3 - b/3! + a^2/8 + ab/8 + b^2/4!;$

$a, b, c < \varepsilon$ $\quad H(1) = \dfrac{1}{3!} - \dfrac{a+b}{8} + (b-c)/4!$
$\quad + [(a+b+c)(4a+3b)$
$\quad + 2a^2 + ab + c^2]/5!;$

(6.3.3.24)

where the nth derivative of $h(x)$ is

$$h_n(x) = (-)^n h(x) - \{(-)^n + n h_{n-1}(x)\}/x. \qquad (6.3.3.25)$$

An alternative method of calculating the scattering power of each Howells polyhedron is based on a subdivision into slices. Within each polyhedron, the loci of constant absorption are planes, equivalent to the dotted lines for the two-dimensional example in Fig. 6.3.3.3. The loci may be determined from the path lengths of rays diffracted at each vertex of the polyhedron. The sum of the path lengths in the incident and diffracted directions is found for each vertex, and the loci determined by interpolation. The slices into which each polyhedron is divided are bounded at the upper and lower faces by planes parallel to the loci of constant absorption, such that at least one vertex of the polyhedron lies on those planes.

The volume of the slice is determined from the coordinates of the vertices on each of the opposite faces. Dummy vertices are inserted if necessary to make the number of vertices on the top and bottom faces identical. For simplicity, an axis (z) is chosen perpendicular to the upper face. This locus of constant absorption with N_v vertices x_i, y_i, z_i has an area

$$D_U = 1/2 \sum_{i=1}^{N_v} (x_i y_{i+1} - y_i x_{i+1}) = E/2. \qquad (6.3.3.26)$$

The corresponding vertices on the lower face may be written $x_i + q\Delta x_i, y_i + q\Delta y_i, z_i + q\Delta z$, with $q = 1$. The lower face has an area

$$D_L = 1/2(E + qF + q^2 G), \quad q = 1, \qquad (6.3.3.27)$$

where

$$F = \sum_{i=1}^{N_v} \Delta x_i y_{i+1} + \Delta y_{i+1} x_i - \Delta x_{i+1} y_i - \Delta y_i x_{i+1}$$

and

$$G = \sum_{i=1}^{N_v} \Delta x_i \, \Delta y_{i+1} - \Delta y_i \, \Delta x_{i+1} \qquad (6.3.3.28)$$

so that the volume of the slice is

$$V_s = 1/2(z_L - z_U)(E + F/2 + G/3). \qquad (6.3.3.29)$$

The diffracting power of an element of the slice, allowing for absorption, is $D(q)\exp(-\mu T)\,\mathrm{d}z$, where T is the total path length of the rays diffracted from this plane. Because of the definition of the Howells polyhedron, the path length

$$T = T_U + q(T_L - T_U) = T_U + q\Delta T. \qquad (6.3.3.30)$$

Thus, the total diffracting power of the slice

$$\begin{aligned} R_s &= 1/2(z_L - z_U)\exp(-\mu T_U) \\ &\quad \times \int_0^1 (E + qF + q^2 G)\exp(-\mu q \Delta T)\,\mathrm{d}q \\ &= 1/2(z_L - z_U)\exp(-\mu T_L)\left\{\frac{-E}{\mu\Delta T} - \frac{F(\mu\Delta T + 1)}{(\mu\Delta T)^2}\right. \\ &\quad \left. - G\frac{(\mu\Delta T^2 + 2\mu\Delta T + 2)}{(\mu\Delta T)^3}\right\} \\ &\quad - 1/2(z_L - z_U)\exp(-\mu T_U)\left\{\frac{-E}{\mu\Delta T} - \frac{F}{(\mu\Delta T)^2} - \frac{2G}{(\mu\Delta T)^3}\right\}. \end{aligned} \qquad (6.3.3.31)$$

The transmission factor for the Howells polyhedron is obtained by summing over the slices, and that for the whole crystal is obtained by summing over the polyhedra, *i.e.*

$$A = \sum R_s \Big/ \sum V_s, \qquad (6.3.3.32)$$

where the crystal volume is $\sum V_s$.

$\mathrm{d}A/\mathrm{d}\mu$, required in calculating $\bar{T}$ for the extinction correction, can be obtained by differentiating R_s for each slice with respect to μ, summing the derivatives for each slice, and dividing by $\sum V_s$. To reduce rounding errors in calculation, it may be desirable to rescale the crystal dimensions so that the path lengths are of the order of unity, multiplying the absorption coefficient by the inverse of the scale factor. Further details are given by Alcock, Pawley, Rourke & Levine (1972).

The number of component tetrahedra or slices, which determines the time and precision required for calculation, is a rapidly increasing function of the number of crystal faces. The method may be computationally prohibitive for crystals with complex shapes.

6.3.3.4. *Gaussian integration*

The integral in the transmission factor in equation (6.3.3.1) may be approximated by a sum over grid points spaced at intervals through the crystal volume. It is usually convenient to orient the grid parallel to the crystallographic axes. The grid is non-isometric, the points being chosen weighted by Gaussian constants to minimize the difference between the weighted sum at those points and the exact value of the integral.

Thus, an integral such as $\int_a^b f(y)\,\mathrm{d}y$ may be approximated (Stroud & Secrest, 1966) by

$$\int_a^b f(y)\,\mathrm{d}y = \frac{b-a}{2}\sum_{i=1}^{n} w_i f(y_i) + R_n, \qquad (6.3.3.33)$$

where

$$y_i = \left(\frac{b-a}{2}\right)X_i + \left(\frac{b+a}{2}\right),$$

X_i is the ith zero of the Legendre polynomial $P_n(X)$,

$$w_i = \frac{2}{(1 - X_i^2)}[P_n'(X_i)]^2, \qquad (6.3.3.34)$$

and

$$R_n = \frac{(b-a)^{2n+1}(n!)^4}{(2n+1)[(2n!)]^3}\, 2^{2n+1} f^{(2n)}(\xi), \quad -1 < \xi < 1. \qquad (6.3.3.35)$$

When applying this to the calculation of a transmission coefficient (Coppens, 1970), we commence with the a-axis grid points x_i selected such that

$$x_i = x_{\min} + (x_{\max} - x_{\min})X_i, \qquad (6.3.3.36)$$

where the X_i are the Gaussian constants.

For each x_i, a line is drawn parallel to **b** and points are then selected such that

$$y_{ij} = y_{\min}(x_i) + [y_{\max}(x_i) - y_{\min}(x_i)]\,X_j. \qquad (6.3.3.37)$$

The procedure is repeated for the c direction, yielding

$$z_{ijk} = z_{\min}(x_i, y_j) + [z_{\max}(s_i, y_j) - z_{\min}(x_i, y_j)]\,X_k. \qquad (6.3.3.38)$$

To calculate the absorption corrections, the incident and diffracted wavevectors are determined. For each grid point, the sum T_{ijk} of the path lengths for the incident and diffracted beams is evaluated. The sum that approximates the transmission coefficient is then

$$A = 1/V \sum_{i,j,k} w_i w_j w_k \exp(-\mu T_{ijk}). \qquad (6.3.3.39)$$

Gaussian constants are tabulated by Abramowitz & Stegun (1964).

Alternative schemes based on Monte Carlo and three-dimensional parabolic integration are described by de Graaff (1973, 1977).

6.3.3.5. *Empirical methods*

Some crystals do not have regular faces, or cannot be measured because these are obscured by the crystal mounting. If corrections based on measurements of the crystal shape are not feasible, absorption measurements may be estimated, either from the intensities of the same reflection at different azimuthal angles ψ (see Subsection 6.3.3.6), or from measurements of equivalent reflections, by empirical methods.

There are variants of the method related to differences in experimental technique. The principles may be illustrated by reference to the procedure for a four-circle diffractometer (Flack, 1977).

Intensities H_m are measurements for a reflection **S** at the angular positions Ω_m, 2θ, χ_m, φ_m. Corrected intensities I_m are to be derived from the measurements by means of a correction factor A_m^* such that

$$I_m = A_m^* H_m. \tag{6.3.3.40}$$

It is assumed that the correction can be written in the form of a rapidly converging Fourier series

$$A_m^* = \sum_{i,j,k,l=-\infty}^{\infty} a_{ijkl}\cos(i\Omega + j2\theta + k\chi + l\varphi) + b_{ijkl}\sin(i\Omega + j2\theta + k\chi + l\varphi). \tag{6.3.3.41}$$

The form of the geometrical terms may be simplified by taking advantage of the symmetry of the four-circle diffractometer. If it is assumed that diffraction is invariant to reversal of the incident and diffracted beams, the settings $\Omega, 2\theta, \chi, \varphi$; $\Omega, -2\theta, -\chi, \pi+\varphi$; $-\Omega, -2\theta, \pi+\chi, \varphi$; $-\Omega, 2\theta, \pi-\chi, \pi+\varphi$; $\pi+\Omega, -2\theta, \chi, \varphi$; $\pi+\Omega, 2\theta, -\chi, \pi+\varphi$; $\pi-\Omega, 2\theta, \pi+\chi, \varphi$; $\pi-\Omega, -2\theta, \pi-\chi, \pi+\varphi$ are equivalent. In shorthand notation, the series (6.3.3.41) reduces to

$$\begin{aligned} A_m^* = \sum a_{\rm cccc} + a_{\rm ccsc} + a_{\rm sccc} + a_{\rm scsc} + a_{\rm sssc} + a_{\rm sscc} \\ + a_{\rm cssc} + a_{\rm cscc} + b_{\rm cccs} + b_{\rm ccss} + b_{\rm sccs} + b_{\rm scss} \\ + b_{\rm ssss} + b_{\rm sscs} + b_{\rm csss} + b_{\rm cscs}. \end{aligned} \tag{6.3.3.42}$$

The range of indices for some terms may be restricted by noting other symmetries in the diffraction experiment. Thus, equation (6.3.3.40) will define the absorption correction for measurements of the incident-beam intensity, with $\Omega = 2\theta = 0$. Since with this geometry the correction will be invariant to rotation about the χ axis, the coefficients for the function involving $\cos(i\Omega)\cos(j2\theta)$ must vanish if the χ index, k, is non-zero. By similar reasoning with the φ axis along the incident beam, one may deduce that coefficients for $\sin(i\Omega)\cos(j2\theta)\sin(k\chi)$ will vanish unless $l = 0$.

Because for a given reflection all measurements are made at the same Bragg angle, the 2θ dependence of the correction cannot be determined by empirical methods. This factor in A is obtained from the absorption correction for a spherical crystal of equivalent radius.

Since an empirical absorption correction is defined only to within a scale factor, the scale must be specified by applying a constraint such that

$$\frac{1}{N_{\rm S}}\sum_{\rm S} A_{\rm S}^* = 1, \tag{6.3.3.43}$$

where $N_{\rm S}$ is the number of independent reflections. Equation (6.3.3.42) may be expressed in the shorthand notation

$$A_{\rm S}^* = \sum_{p=0} C_p f_{p\rm S}, \tag{6.3.3.44}$$

where C_p is the coefficient in a term such as $a_{\rm ccsc}$ or $b_{\rm ccss}$ and $f_{p\rm S}$ is the corresponding geometrical function. Labelling the constant geometrical term with a value of unity as f_0 and rearranging leads to

$$A_{\rm S}^* = 1 + \sum_{p=1} C_p\left\{f_{p\rm S} - \frac{1}{N_{\rm S}}\sum_{\rm S} f_{p\rm S}\right\} = 1 + \sum_{p=1} C_p g_{p\rm S}, \tag{6.3.3.45}$$

which defines $g_{p\rm S}$.

Equation (6.3.3.40) is now expressed as

$$I_{m\rm S} = H_{m\rm S} + H_{m\rm S}\sum_{p=1} C_p g_{p\rm S}, \tag{6.3.3.46}$$

in which the coefficients C_p are to be chosen so that the values of $I_{m\rm S}$ for each **S** are as near equal as possible. Since the values within each set will not be exactly equal, we rewrite (6.3.3.46) as

$$\Delta_{m\rm S} - H_{m\rm S} = -I_{\rm S} + H_{m\rm S}\sum_{p=1} C_p g_{p\rm S}, \tag{6.3.3.47}$$

in which the mean intensity $I_{\rm S}$ and the C_p are chosen to minimize $\sum_{{\rm S},m} w_{\rm S}^2\Delta_{m\rm S}^2$, where

$$\Delta_{m\rm S} = I_{m\rm S} - I_{\rm S}, \tag{6.3.3.48}$$

and $w_{\rm S}$ is the weight for that reflection.

If the equation to be solved

$$-w_{\rm S}H_{m\rm S} \simeq -w_{\rm S}I_m + \sum_{p=1} C_p g_{p\rm S} w_{\rm S} I_{m\rm S} \tag{6.3.3.49}$$

is written in the shorthand form

$$\boldsymbol{D} = \boldsymbol{F}\boldsymbol{C}, \tag{6.3.3.50}$$

in which $\boldsymbol{D}$ corresponds to $-w_{\rm S}H_{m\rm S}$, the I_m and C_p correspond to $\boldsymbol{C}$, with $(-w_{\rm S})$ and $w_{\rm S}g_{p\rm S}H_{m\rm S}$ corresponding to $\boldsymbol{F}$, the solution to (6.3.3.50) can be determined from the normal equations

$$\boldsymbol{C} = (\boldsymbol{F}^T\boldsymbol{F})^{-1}\boldsymbol{F}^T\boldsymbol{D}, \tag{6.3.3.51}$$

where $\boldsymbol{F}^T$ is the transpose of $\boldsymbol{F}$. This procedure suffers from the disadvantages of requiring a matrix inversion whenever the set of trial functions (*i.e.* those multiplied by the coefficients C_p) is modified. The tedious inversion of the normal equations, described by (6.3.3.51), may be replaced by a simple inversion *via* the Gram–Schmidt orthogonalizing process, *i.e.* by calculating a matrix $\boldsymbol{W}$ with mutually orthogonal columns $\boldsymbol{W}_j$ such that

$$\begin{aligned} \boldsymbol{W}_1 &= \boldsymbol{F}_1 \\ \boldsymbol{W}_j &= \boldsymbol{F}_j - \sum_{k=1}^{j-1}(\boldsymbol{F}_j\cdot\boldsymbol{W}_k)\boldsymbol{W}_k/\boldsymbol{W}_k^2. \end{aligned} \tag{6.3.3.52}$$

The minimizing of $(\boldsymbol{D}-\boldsymbol{F}\boldsymbol{C})^2$ is replaced by minimizing $(\boldsymbol{D}-\boldsymbol{W}\boldsymbol{A})^2$. Differentiating with respect to a_j yields

$$a_j = \frac{\boldsymbol{D}\cdot\boldsymbol{W}_j}{\boldsymbol{W}_j^2}. \tag{6.3.3.53}$$

If equation (6.3.3.52) is written as

$$\boldsymbol{F} = \boldsymbol{W}\boldsymbol{B},$$

where the upper triangular matrix $\boldsymbol{B}$ is

$$b_{ij} = \boldsymbol{F}_j \cdot \boldsymbol{W}_i / \boldsymbol{W}_i^2, \quad i < j; \quad b_{ij} = 1, i = j; \quad b_{ij} = 0, i > j, \tag{6.3.3.54}$$

the vector determining the coefficients is

$$\boldsymbol{C} = \boldsymbol{B}^{-1}\boldsymbol{A}, \tag{6.3.3.55}$$

in which the inversion of $\boldsymbol{B}$ is straightforward.

In difficult cases, with data affected by errors in addition to absorption, the method described may give physically unreasonable absorption corrections for some reflections. In such cases, it may help to impose the approximate constraints

$$\sum_{\mathbf{S}} w_{\mathbf{S}}^2 H_{m\mathbf{S}} \Big/ \sum_{\mathbf{S}} w_{\mathbf{S}}^2 = \sum_{\mathbf{S}} w_{\mathbf{S}}^2 I_{m\mathbf{S}} \Big/ \sum_{\mathbf{S}} w_{\mathbf{S}}^2. \tag{6.3.3.56}$$

If $m = 1, 2, \ldots, M$, this reduces to the M constraint equations

$$\sum_{p=1} C_p \left\{ \frac{\sum_{\mathbf{S}} w_{\mathbf{S}}^2 H_{m\mathbf{S}} g_{p\mathbf{S}}}{\sum_{\mathbf{S}} w_{\mathbf{S}}^2} \right\} = \sum_{p=1} C_p \left\{ \frac{\varepsilon w_m \sum_{\mathbf{S}} w_{\mathbf{S}}^2 H_{m\mathbf{S}} g_{p\mathbf{S}}}{\sum_{\mathbf{S}} w_{\mathbf{S}}^2} \right\} = 0, \tag{6.3.3.57}$$

where w_m is the square root of the weight for the weighted mean of the equivalent reflections H_m, defined as

$$H_m = \sum_{\mathbf{S}} w_{\mathbf{S}}^2 H_{m\mathbf{S}} \Big/ \sum_{\mathbf{S}} w_{\mathbf{S}}^2 \quad \text{for each } \mathbf{S}, \tag{6.3.3.58}$$

and the multiplier ε controls the strength with which the additional constraints are enforced. With the additional constraint equations, the sum of squares to be minimized, corresponding to (6.3.3.48), becomes

$$\sum_{\mathbf{S},m} w_{\mathbf{S}}^2 (I_{m\mathbf{S}} - I_m)^2 + \sum_{m} \varepsilon^2 w_m^2 (H_m - I_m)^2. \tag{6.3.3.59}$$

A closely related procedure expressing the absorption corrections as Fourier series in polar angles for the incident and diffracted beams is described by Katayama, Sakabe & Sakabe (1972). A similar method minimizing the difference between observed and calculated structure factors is described by Walker & Stuart (1983). Other experimental techniques for measuring data for empirical absorption corrections that could be analysed by the Fourier-series method are described by Kopfmann & Huber (1968), North, Phillips & Mathews (1968), Flack (1974), Stuart & Walker (1979), Lee & Ruble (1977*a*,*b*), Schwager, Bartels & Huber (1973), and Santoro & Wlodawer (1980).

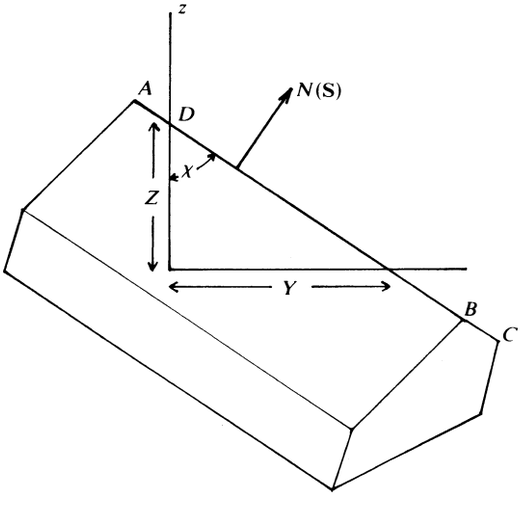

Fig. 6.3.3.4. Crystal oriented with the normal $N(\mathbf{S})$ to the face *ABCD* in the plane of view.

6.3.3.6. *Measuring crystals for absorption*

In general, A depends both on the shape of the crystal and on its orientation with respect to the incident and diffracted beams. To measure the shape of the crystal, a measuring microscope is mounted in the xy plane, and the crystal rotated about the z axis at right angles to that plane. A rotation about the z axis changes the orientation of the crystal x and y coordinates with respect to those (X and Y) for the measuring device. The x axis is directed from crystal to microscope when the angle of rotation about the z axis (φ) is zero. During rotation, each face will at some stage be oriented with its normal $N(\mathbf{S})$ perpendicular to the line of view, *i.e.* in the XY plane for instrument coordinates. If the angle of rotation at that orientation is denoted φ_N, the appearance of a typical face *ABCD* will be as indicated in Fig. 6.3.3.4.

The equation for the plane is

$$x \sin\varphi_N + y \cos\varphi_N + z \tan\chi = Y$$

or, equivalently,

$$(x \sin\varphi_N + y \cos\varphi_N) \cot\chi + z = Z.$$

For a crystal oriented on an Eulerian cradle, it is necessary to specify the orientation of the crystal, *i.e.* the angles Ω, χ, φ in which the measurements of the diffraction intensities are made. In a reflecting position, the reciprocal-lattice vector $\mathbf{S}$, which is normal to the Bragg planes, bisects the angle between the incident and diffracted beams, as shown in Fig. 6.3.3.5.

If the crystal is rotated about the reciprocal-lattice vector $\mathbf{S}$, varying the angle ψ, the crystal remains in a reflecting position. That is, there is a degree of freedom in the scattering experiment that enables the same reflection to be observed at different sets of Ω, χ, φ values. The path length varies with ψ, except for spherical crystals. In order to calculate an absorption correction, the value of ψ and its origin must be specified. For a crystal mounted on an Eulerian cradle, the bisecting position, with $\Omega = \theta$, is usually chosen as the origin for ψ.

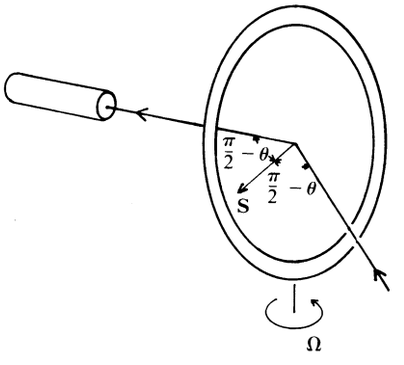

Fig. 6.3.3.5. Geometry of the Eulerian cradle in the bisecting position.

6.2 (*cont.*)

Werner, S. A. & Arrott, A. (1965). *Propagation of Bragg-reflected neutrons in large mosaic crystals and the efficiency of monochromators*. *Phys. Rev.* **140**, A675–A686.

Werner, S. A., Arrott, A., King, J. S. & Kendrick, H. (1966). *Propagation of Bragg-reflected neutrons in bounded mosaic crystals*. *J. Appl. Phys.* **37**, 2343–2350.

6.3

Abramowitz, M. & Stegun, I. A. (1964). *Handbook of mathematical functions*, p. 916. National Bureau of Standards Publication AMS 55.

Alcock, N. W., Pawley, G. S., Rourke, C. P. & Levine, M. R. (1972). *An improvement in the algorithm for absorption correction by the analytical method*. *Acta Cryst.* A**28**, 440–444.

Anderson, D. W. (1984). *Absorption of ionizing radiation*. Baltimore: University Park Press.

Azaroff, L. V., Kaplow, R., Kato, N., Weiss, R. J., Wilson, A. J. C. & Young, R. A. (1974). *X-ray diffraction*, pp. 282–284. New York: McGraw-Hill.

Becker, P. J. & Coppens, P. (1974). *Extinction within the limit of validity of the Darwin transfer equations. I. General formalisms for primary and secondary extinction and their application to spherical crystals*. *Acta Cryst.* A**30**, 129–147.

Beeman, W. W. & Friedman, H. (1939). *The X-ray K absorption edges of the elements Fe (26) to Ge (32)*. *Phys. Rev.* **56**, 392–405.

Coppens, P. (1970). *The evaluation of absorption and extinction in single crystal structure analysis*. *Crystallographic computing*, edited by F. R. Ahmed, S. R. Hall & C. P. Huber, pp. 255–270. Copenhagen: Munksgaard.

Coyle, B. A. (1972). *Absorption and volume corrections for a cylindrical specimen, larger than the beam, and in general orientation*. *Acta Cryst.* A**28**, 231–233.

Coyle, B. A. & Schroeder, L. W. (1971). *Absorption and volume corrections for a cylindrical sample, larger than the X-ray beam, employed in Eulerian geometry*. *Acta Cryst.* A**27**, 291–295.

Dwiggins, C. W. Jr (1975*a*). *Rapid calculation of X-ray absorption correction factors for cylinders to an accuracy of 0.1%*. *Acta Cryst.* A**31**, 146–148.

Dwiggins, C. W. Jr (1975*b*). *Rapid calculation of X-ray absorption correction factors for spheres to an accuracy of 0.05%*. *Acta Cryst.* A**31**, 395–396.

Flack, H. D. (1974). *Automatic absorption correction using intensity measurements from azimuthal scans*. *Acta Cryst.* A**30**, 569–573.

Flack, H. D. (1977). *An empirical absorption–extinction correction technique*. *Acta Cryst.* A**33**, 890–898.

Flack, H. D. & Vincent, M. G. (1978). *Absorption weighted mean path lengths for spheres*. *Acta Cryst.* A**34**, 489–491.

Fukamachi, T., Karamura, T., Hayakawa, K., Nakano, Y. & Koh, F. (1982). *Observation of effect of temperature on X-ray diffraction intensities across the In K absorption edge of InSb*. *Acta Cryst.* A**38**, 810–813.

Graaff, R. A. G. de (1973). *A Monte Carlo method for the calculation of transmission factors*. *Acta Cryst.* A**29**, 298–301.

Graaff, R. A. G. de (1977). *On the calculation of transmission factors*. *Acta Cryst.* A**33**, 859.

James, R. W. (1962). *The optical principles of the diffraction of X-rays*, pp. 135–192. Ithaca: Cornell University Press.

Karamura, T. & Fukamachi, T. (1979). *Temperature dependence of X-ray reflection intensity from an absorbing perfect crystal near an absorption edge*. *Acta Cryst.* A**35**, 831–835.

Katayama, C., Sakabe, N. & Sakabe, K. (1972). *A statistical evaluation of absorption*. *Acta Cryst.* A**28**, 293–295.

Kopfmann, G. & Huber, R. (1968). *A method of absorption correction for X-ray intensity measurements*. *Acta Cryst.* A**24**, 348–351.

Krause, M. O. & Oliver, J. H. (1979). *Natural widths of atomic K and L levels, Kα X-ray lines and several KLL Auger lines*. *J. Phys. Chem. Ref. Data*, **8**, 329–338.

Lee, B. & Ruble, J. R. (1977*a*). *A semi-empirical absorption-correction technique for symmetric crystals in single-crystal X-ray crystallography. I.* *Acta Cryst.* A**33**, 629–637.

Lee, B. & Ruble, J. R. (1977*b*). *A semi-empirical absorption-correction technique for symmetric crystals in single-crystal X-ray crystallography. II.* *Acta Cryst.* A**33**, 637–641.

North, A. C. T., Phillips, D. C. & Mathews, F. S. (1968). *A semi-empirical method of absorption correction*. *Acta Cryst.* A**24**, 351–359.

Rigoult, J. & Guidi-Morosini, C. (1980). *An accurate calculation of $\bar{T}_\mu$ for spherical crystals*. *Acta Cryst.* A**36**, 149–151.

Rouse, K. D., Cooper, M. J., York, E. J. & Chakera, A. (1970). *Absorption corrections for neutron diffraction*. *Acta Cryst.* A**26**, 682–691.

Santoro, A. & Wlodawer, A. (1980). *Absorption corrections for Weissenberg diffractometers*. *Acta Cryst.* A**36**, 442–450.

Schwager, P., Bartels, K. & Huber, R. (1973). *A simple empirical absorption-correction method for X-ray intensity data films*. *Acta Cryst.* A**29**, 291–295.

Stroud, A. H. & Secrest, D. (1966). *Gaussian quadrature formulas*. New Jersey: Prentice-Hall.

Stuart, D. & Walker, N. (1979). *An empirical method for correcting rotation-camera data for absorption and decay effects*. *Acta Cryst.* A**35**, 925–933.

Templeton, D. H. & Templeton, L. K. (1980). *Polarized X-ray absorption and double refraction in vanadyl bisacetylacetonate*. *Acta Cryst.* A**36**, 237–241.

Templeton, D. H. & Templeton, L. K. (1982). *X-ray dichroism and polarized anomalous scattering of the uranyl ion*. *Acta Cryst.* A**38**, 62–67.

Templeton, D. H. & Templeton, L. K. (1985). *Tensor optical properties of the bromate ion*. *Acta Cryst.* A**41**, 133–142.

Tibballs, J. E. (1982). *The rapid computation of mean path lengths for cylinders and spheres*. *Acta Cryst.* A**38**, 161–163.

Wagenfeld, H. (1975). *Theoretical computations of X-ray dispersion corrections*. *Anomalous scattering*, edited by S. Ramaseshan & S. C. Abrahams, pp. 13–24. Copenhagen: Munksgaard.

Walker, N. & Stuart, D. (1983). *An empirical method for correcting diffractometer data for absorption effects*. *Acta Cryst.* A**39**, 158–166.

Weber, K. (1969). *Eine neue Absorptionsfactortafel für kugelförmige Proben*. *Acta Cryst.* B**25**, 1174–1178.

Zachariasen, W. H. (1968). *Extinction and Borrmann effect in mosaic crystals*. *Acta Cryst.* A**24**, 421–424.